

7. T. Shuin *et al.*, *Cancer Res.* **54**, 2852 (1994).
8. H. Kanno *et al.*, *ibid.*, p. 4845.
9. J. G. Herman *et al.*, *Proc. Natl. Acad. Sci. U.S.A.* **91**, 9700 (1994).
10. J. R. Gnarr *et al.*, *Nat. Genet.* **7**, 85 (1994).
11. O. Iliopoulos, A. Kibel, S. Gray, W. G. Kaelin, *Nat. Med.* **1**, 822 (1995).
12. The Bam HI-Eco RI *VHL* cDNA fragment from pSP72-VHL(BZ3-4) (17) was ligated into pSG5 (Stratagene) to create pSG5-VHL(AB6-2). A C to T change was introduced (24) at *VHL* nucleotide position 712, to create pSG5-VHL(167W). A Bst EII-Eco RI *VHL* cDNA fragment from this plasmid was used to shuttle this mutation into pcDNA-HAVHL (17) to create pcDNA-HAVHL(167W). The Hind III-Xba I *VHL* cDNA fragment was ligated into pRc/CMV (Invitrogen) to create pRc-HAVHL(167W).
13. Immunoprecipitations and GST-binding experiments were performed as in (25, 26), except that the Sepharose was washed four times with NETN(960) [20 mM tris-HCl (pH 8.0), 960 mM NaCl, 1 mM EDTA, 0.5% Nonidet P-40] and once with NETN (no NaCl) before addition of sample buffer. For immunoprecipitations, pRc-HAVHL cell lines were labeled with 500 μ Ci/ml of Expre^{35S}35S protein labeling mix (New England Nuclear) for 4 hours. The 293, ACHN, CAKI-1, and parental 786-O cells were labeled with 1 mCi/ml of this mix for 4 hours. Each immunoprecipitation reaction contained equivalent amounts of cell extract, derived from ~50% of the adherent cells in a nearly confluent 100-mm dish. For GST-binding experiments, parental 786-O cells were labeled with 500 μ Ci/ml of the labeling mix for 4 hours. Each reaction contained equivalent amounts of cell extract derived from approximately one-eighth of the adherent cells in a nearly confluent 100-mm dish.
14. BNR 5.12 mice were immunized with purified GST-pVHL(1-213) with Freund's complete and incomplete adjuvants, and monoclonal hybridoma cells were prepared. IG32 is an IgG1 that reacts with pVHL in both immunoblot and immunoprecipitation assays. Anti-HA (12CA5) (27) and control [anti-RBAP2 (LY11)] (28) antibodies have been described previously. Immunoprecipitations were performed with 50 μ l of hybridoma supernatant without a secondary antibody. The anti-HA supernatant was diluted 1:50 (v/v) for immunoblot analysis.
15. Segments of the *VHL* cDNA were amplified by the polymerase chain reaction (PCR) with sense and antisense primers containing Bam HI and Eco RI sites, respectively. The products were digested and ligated into pGEX2TK (28).
16. A. Kibel, O. Iliopoulos, W. G. Kaelin Jr., unpublished observations.
17. *VHL* peptides were made with an Applied Biosystems (ABI) synthesizer and dissolved (5 mg/ml) in phosphate-buffered saline with 1 mM dithiothreitol.
18. D. R. Duan *et al.*, *Proc. Natl. Acad. Sci. U.S.A.* **92**, 6459 (1995).
19. After SDS-PAGE, proteins were transferred to a PVDF membrane [Probot (ABI)] in 0.5 \times Towbin Buffer [12.5 mM tris-HCl (pH 8.0), 96 mM glycine, 10% methanol] and stained with amido black. The filter was destained and p18 was excised and digested with trypsin (29, 30). The peptides were separated by narrow-bore high-performance liquid chromatography (HPLC). Selected peptide fractions were subjected to automated Edman degradation on an ABI 477A or 494A (30).
20. D. R. Duan *et al.*, *Science* **269**, 1402 (1995); T. Aso, W. S. Lane, J. W. Conaway, R. C. Conaway, *ibid.*, p. 1439.
21. K. Garrett *et al.*, *Proc. Natl. Acad. Sci. U.S.A.* **92**, 7172 (1995).
22. K. Garrett, D. Haque, R. Conaway, J. Conaway, *Gene* **150**, 413 (1994).
23. K. Garrett *et al.*, *Proc. Natl. Acad. Sci. U.S.A.* **91**, 5237 (1994).
24. K. Foss and W. H. McClain, *Gene* **59**, 285 (1987).
25. W. G. Kaelin, D. C. Pallas, J. A. DeCaprio, F. J. Kaye, D. M. Livingston, *Cell* **64**, 521 (1991).
26. J. A. DeCaprio *et al.*, *ibid.* **54**, 275 (1988).
27. J. Field *et al.*, *Mol. Cell. Biol.* **8**, 2129 (1988).
28. W. G. Kaelin *et al.*, *Cell* **70**, 351 (1992).
29. J. Fernandez, M. DeMott, D. Atherton, S. M. Mische, *Anal. Biochem.* **201**, 255 (1992).
30. W. S. Lane, A. Galat, M. W. Harding, S. L. Schreiber, *J. Prot. Chem.* **10**, 151 (1991).
31. We thank R. Klausner, R. C. Conaway, J. W. Conaway, and their colleagues for graciously sharing their data with us prior to publication; R. Klausner for p18 and p14 translated in vitro; V. Bailey and W. Lane for the HPLC, mass spectrometry, and peptide sequencing; J. Gan for help with anti-VHL; C. Nalin for the pVHL peptides; B. Zbar for help in compiling the published data on *VHL* germline mutations; and

M. Modabber, T. Garelik, and their colleagues for illustrations and helpful comments. A. K. thanks J. Richie for encouragement and support. O.I. is an American Society of Clinical Oncology Fellow and is supported by the Irving Janick Fund. W.G.K. is a McDonnell Foundation Scholar and is supported by an NIH Physician-Scientist Award and the Sandoz Research Institute.

18 July 1995; accepted 15 August 1995

Decreased Muscarinic Receptor Binding in the Arcuate Nucleus in Sudden Infant Death Syndrome

Hannah C. Kinney,* James J. Filiano,† Lynn A. Sleeper, Frederick Mandell, Marie Valdes-Dapena, W. Frost White

Muscarinic cholinergic activity in the human arcuate nucleus at the ventral medullary surface is postulated to be involved in cardiopulmonary control. A significant decrease in [³H]quinuclidinyl benzilate binding to muscarinic receptors in the arcuate nucleus is now shown to occur in sudden infant death syndrome (SIDS) infants, compared to infants dying acutely of known causes. In infants with chronic oxygenation abnormalities, binding is low in other nuclei, as well as in the arcuate nucleus. The binding deficit in the arcuate nucleus of SIDS infants might contribute to a failure of responses to cardiopulmonary challenges during sleep.

Sudden infant death syndrome is the leading cause of postneonatal infant death in the United States. SIDS is defined as the sudden death of an infant under 1 year of age that remains unexplained after a thorough case investigation, including performance of a complete autopsy, examination of the death scene, and review of the clinical history (1). The syndrome is temporally associated with sleep periods, resulting in the premise that SIDS occurs during sleep or during transitions between sleep and waking. Recent epidemiologic data have shown a positive association between prone sleeping position and SIDS incidence, and decreased SIDS rates have been reported in countries that have initiated intervention programs advocating a supine sleeping position (2). The mechanism for the association between decreased prone prevalence and decreased risk for SIDS is unknown, but

an interaction possibly exists between prone position and impaired cardioventilatory control, particularly impaired ventilatory and arousal responsiveness (3).

We hypothesize that SIDS, or a subset of SIDS, is associated with a deficiency in muscarinic cholinergic receptor (mAChR) binding in the arcuate nucleus of the ventral surface of the medulla (ventral medullary surface, VMS), which results in an impaired response to hypercarbia or asphyxia during sleep and sudden death. In animals, the precise location of the chemosensors is debated, but there is substantial evidence that the VMS participates in the ventilatory response to carbon dioxide (CO₂) and hydrogen ion, cardioventilatory coupling, and pressor responses (4). VMS cells are intimately associated with ventrolateral neurons of the brainstem that integrate ventilatory, pressor, and defense responses (5, 6). The precise function or functions of the human arcuate nucleus is speculative, as it is not possible to perform direct experiments ablating or stimulating arcuate neurons in living humans. In a previous study comparing the anatomy of the VMS in human infants and cats, we found that the arcuate nucleus is anatomically homologous to a distinct cell population in the cat VMS (7). We also reported a subset of SIDS infants with a severe developmental hypoplasia of the arcuate nucleus (8). The hypothesis that arcuate neurons are VMS cell populations involved in the response to hypercarbia in humans is supported by functional magnetic resonance imag-

H. C. Kinney, Departments of Pathology and Neurology, Children's Hospital and Harvard Medical School, Boston, MA 02115, USA.

J. J. Filiano, Department of Neurology, Children's Hospital and Harvard Medical School, Boston, MA 02115, USA.

L. A. Sleeper, New England Research Institutes, Watertown, MA 02172, USA.

F. Mandell, Department of Pediatrics, Children's Hospital and Harvard Medical School, Boston, MA 02115, USA.

M. Valdes-Dapena, Department of Pathology, University of Miami School of Medicine, Miami, FL 33101, USA.

W. F. White, Department of Neuroscience, Pfizer Central Research, Groton, CT 06340, USA.

*To whom correspondence should be addressed.

†Present address: Department of Pediatrics, Children's Hospital at Dartmouth, Dartmouth Hitchcock Medical Center, Lebanon, NH 03756, USA.

ing in adults exposed to hypercarbia in which CO₂ responsivity is localized to the region of the arcuate nucleus (9), and by a case report of an infant with congenital central hypoventilation syndrome and absence of the arcuate nucleus at autopsy (10). Acetylcholine has been implicated experimentally in mediating the ventilatory response to CO₂ and hydrogen ion via mAChRs at the VMS (11, 12), and mAChR binding has been shown to localize extensively to the human arcuate nucleus, the only nucleus along the VMS in humans with appreciable muscarinic binding (13, 14). In the present study, we have used tissue receptor autoradiography to test the hypothesis that the binding of the muscarinic antagonist [³H]quinuclidinyl benzilate ([³H]QNB) is deficient (decreased) in the arcuate nucleus in SIDS infants.

Brainstems from a total of 77 cases were analyzed: 45 SIDS, 14 acute controls, and 18 infants in a chronic group (15). The acute controls were infants who were completely well or had recognized illnesses prior to death and who died suddenly and unexpectedly; a complete autopsy established a cause of death (16). The chronic group was composed of infants with a history of chronic or repetitive hypoxemia from cardiac, pulmonary, or central breathing disorders (17). The purpose of the analysis of the chronic group with oxygenation or breathing disorders was to address the possibility that the putative mAChR binding defect in the arcuate nucleus in SIDS infants is not specific, but rather reflects an effect of hypoxia-ischemia. Comparison of the SIDS and acute control groups showed no significant differences between mean gestational age, birth weight, and Apgar scores, or between rates of complications of pregnancy,

labor, or postnatal course, oxygen use in the delivery room, or history of an apparent life-threatening event (18).

We assessed [³H]QNB binding to mAChRs with quantitative tissue receptor autoradiography (Fig. 1) (13, 19, 20). QNB

Table 1. Age-adjusted muscarinic binding means \pm SEM (fmol/mg tissue) for 17 nuclei. Analysis of covariance (ANCOVA) was used to examine differences in binding by diagnosis, adjusted for postconceptional age (the covariate) (24). Postmortem interval was not used as an additional covariate because, although it differed slightly on average by diagnosis, it was not significantly correlated with [³H]QNB binding in this data set. When the relation between age and binding was similar for the three groups, age-adjusted mean binding levels were estimated for the three groups on the basis of the mean age of the entire sample (24). When the ANCOVA *P* value for case diagnosis was less than 0.05, signifying differences in mean binding among the three groups, pairwise comparisons of the age-adjusted means were conducted. The number of samples is indicated in parentheses. n., nucleus; Bands, paramedian bands in rostral pontine reticular formation (13); IPN, interpeduncular nucleus.

Site	SIDS	Acute	Chronic	<i>P</i> (three-group)
Arcuate n.	110 \pm 6 (44)	150 \pm 12 (14)	111 \pm 11 (18)	0.012*
Basis pontis	276 \pm 10 (43)	275 \pm 18 (14)	234 \pm 18 (16)	0.138
Inferior olive	70 \pm 4 (43)	68 \pm 7 (13)	64 \pm 6 (18)	0.695
Hypoglossal n.	314 \pm 13 (41)	295 \pm 24 (12)	224 \pm 22 (15)	0.003†
n. Tractus solitarii	180 \pm 8 (41)	161 \pm 15 (12)	152 \pm 12 (17)	0.432
n. Centralis	138 \pm 4 (44)	125 \pm 7 (14)	140 \pm 7 (18)	0.244
n. Gigantocellularis	137 \pm 5 (41)	127 \pm 9 (11)	132 \pm 7 (18)	0.559
n. Paragigantocellularis	113 \pm 4 (39)	109 \pm 7 (11)	109 \pm 6 (18)	0.792
n. Parabrachialis medialis	147 \pm 7 (22)	156 \pm 17 (4)	135 \pm 13 (9)	0.605
n. Parabrachialis lateralis	125 \pm 5 (35)	129 \pm 9 (10)	116 \pm 9 (13)	0.571
n. Pontis oralis	145 \pm 5 (34)	139 \pm 9 (12)	127 \pm 9 (14)	0.210
Locus coeruleus	155 \pm 6 (31)	163 \pm 11 (10)	146 \pm 10 (14)	0.553
Bands	205 \pm 8 (34)	213 \pm 13 (11)	155 \pm 14 (11)	0.008‡
IPN	276 \pm 13 (31)	251 \pm 21 (12)	245 \pm 25 (9)	0.385
n. Cuneiformis	161 \pm 6 (24)	158 \pm 9 (13)	161 \pm 10 (10)	0.954
n. Raphe dorsalis	162 \pm 9 (21)	153 \pm 13 (10)	160 \pm 17 (6)	0.863
Inferior colliculus	230 \pm 13 (17)	231 \pm 18 (9)	242 \pm 20 (8)	0.874

*SIDS differ from acute controls (*P* = 0.003) and chronic groups differ from acute controls (*P* = 0.026). Raw means \pm SEM: SIDS, 110 \pm 6 fmol/mg tissue; acute, 153 \pm 13 fmol/mg tissue; chronic 108 \pm 10 fmol/mg. †Chronics differ from SIDS (*P* < 0.001) and chronics differ from acute (*P* = 0.034). ‡Chronics differ from SIDS (*P* = 0.003) and chronics differ from acute (*P* = 0.006).

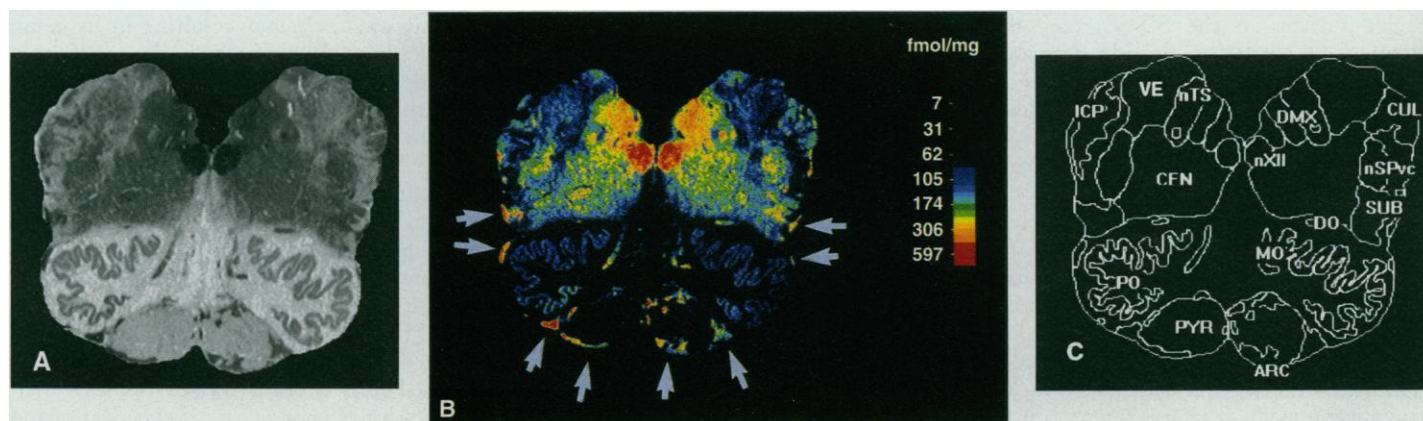


Fig. 1. The [³H]QNB binding procedure used in the present study for tissue receptor autoradiography was based on methods developed in experimental animals (19) and applied in human postmortem pediatric brain tissues (13, 14, 20). (A) Autoradiogram of representative level of the medulla. The arcuate nucleus is located along the ventral surface, overlying the pyramid. (B) Color-coded image of specific activity (fmol/mg tissue) in same section. The white arrows point to the arcuate nucleus. (C) Anatomic boundaries of nuclei. ARC,

arcuate nucleus; CEN, nucleus centralis; CUL, nucleus cuneatus lateralis; DMX, dorsal motor nucleus of the vagus; DO, dorsal accessory olive; ICP, inferior cerebellar peduncle; MO, medial accessory olive; nXI, hypoglossal nucleus; nSPvc, nucleus of the spinal trigeminal nerve, pars caudalis; nTS, nucleus tractus solitarii; PO, principal inferior olive; PYR, pyramid; SUB, nucleus subtrigeminalis; VE, vestibular nucleus.

is a potent antagonist that binds nonspecifically to all of the pharmacologically defined mAChRs and to the human m1-4 subtypes (13). We analyzed mean muscarinic binding in each of the 17 nuclei (Table 1). We also analyzed the ratio of muscarinic binding in each of the 17 nuclei to that in four sites: (i) basis pontis, (ii) inferior olive, (iii) hypoglossal nucleus, and (iv) nucleus gigantocellularis (Table 2). The ratio analyses were used to correct for overall variation in binding among cases. The four nuclei were chosen because (i) the basis pontis (cerebellar relay) is a region that is not directly related to autonomic or ventilatory control and is one of two sites with the highest [³H]QNB binding in the infant brainstem; (ii) the hypoglossal nucleus (upper airway control) is the other site of highest [³H]QNB binding in the infant brainstem; (iii) the inferior olive (cerebellar relay) is the nucleus with the lowest mAChR binding in all cases; and (iv) the nucleus gigantocellularis (reticular formation) has an intermediate level of binding.

Of the 17 regions analyzed throughout the brainstem, the arcuate nucleus was the only region in which there was a significant difference in age-adjusted mean binding between the SIDS and acute control groups (Fig. 2 and Table 1). The differences in mAChR binding remained significant after adjustment for postmortem interval (three-group, $P = 0.016$; SIDS versus acute, $P = 0.005$). The age-adjusted mean binding for the arcuate nucleus was similar for the SIDS and chronic groups, and like the SIDS group, was significantly different from that of acute controls (Table 1). This observation raised the possibility that decreased mAChR binding in the arcuate nucleus in the SIDS group was secondary to oxygenation or breathing abnormalities. However, in contrast to the specific decrease in mAChR binding in the arcuate nucleus in the SIDS group, the chronic group had significantly decreased binding compared with acute controls in three brainstem nuclei: the arcuate nucleus, the hypoglossal nucleus, and a subdivision of the rostral pontine reticular formation (paramedian muscarinic bands).

In three of the ratio analyses (:nucleus gigantocellularis; :hypoglossal nucleus; :inferior olive), mean age-adjusted binding in the arcuate nucleus differed significantly among the three groups (three-group: $P = 0.013$, $P < 0.001$, $P = 0.033$, respectively). In contrast, the basis pontis ratio analysis revealed a significant age-by-diagnosis interaction ($P = 0.043$); the correlation between age and binding in the chronic group differed from the correlation observed for the SIDS and acute groups. Nevertheless, in this ratio analysis, as well as in the other three, the SIDS group had significantly lower mean binding than the acute control group (Table 2).

Table 2. Age-adjusted mean mAChR binding of SIDS and control groups. Postconceptional age-adjusted mean \pm SEM are shown. The ratio analyses were used to correct for overall variation in binding among cases: the ratio of the binding of each site to the binding of the basis pontis, nucleus gigantocellularis, hypoglossal nucleus, and inferior olive was analyzed, with these four nuclei serving as internal standards. The age-adjusted means of the untransformed ratio measurements are presented for ease of interpretation, along with P values from the log-transformed analyses. The ratio values were log-transformed to meet normality assumptions of the regression model. Asterisk denotes age-adjusted means for ARC/BP based on a submodel that excludes the chronic group, due to a significant interaction with age (mAChR binding of the chronic group decreases with age; binding of SIDS and acute controls does not vary with age). The number of samples is indicated in parentheses. ARC, arcuate nucleus; BP, basis pontis; GC, nucleus gigantocellularis; HN, hypoglossal nucleus; IO, inferior olive.

Ratio	SIDS	Acute	Chronic	P (SIDS versus acute)	P (chronic versus acute)
ARC/BP	0.42 \pm 0.03 (43)	0.56 \pm 0.05 (14)	* (16)	0.012	*
ARC/GC	0.84 \pm 0.31 (41)	1.26 \pm 0.44 (11)	0.79 \pm 0.29 (17)	0.003	0.035
ARC/HN	0.36 \pm 0.13 (41)	0.57 \pm 0.25 (12)	0.51 \pm 0.16 (14)	0.002	0.777
ARC/IO	1.63 \pm 0.54 (43)	2.34 \pm 1.11 (13)	1.73 \pm 0.64 (17)	0.010	0.137

There was also an age-by-diagnosis interaction in the binding ratios for the nucleus raphe dorsalis to the hypoglossal nucleus and to the nucleus gigantocellularis. The binding ratio in the acute group decreased significantly with age (0.03 to 0.04 fmol of tissue per milligram per week), whereas the binding ratio in the SIDS group increased slightly with age (0.01 fmol of tissue per milligram per week). Therefore, the mean difference in binding ratios between the SIDS and acute control groups is age-dependent. The nucleus raphe dorsalis was not a focus of our original research, and the significance of these findings is unclear and requires further study. At several sites, group differences in binding ratios with the basis pontis and nucleus gigantocellularis depended on age, but in each instance this was due to the chronic group differing from the SIDS and acute control groups, which were not significantly different from each other.

We found several significant chronic versus acute control differences in mAChR binding ratios. Compared to the acute group, the chronic group had significantly lower nucleus gigantocellularis binding ratios at three sites: the arcuate nucleus, hypoglossal nucleus, and paramedian bands, the same sites that had significantly decreased mean binding values. The hypoglossal nucleus ratio analyses revealed five other sites where the chronic group ratios differed significantly from the acute controls: nucleus tractus solitarius, nucleus centralis, nucleus gigantocellularis, nucleus paragigantocellularis lateralis, and nucleus cuneiformis. Although the underlying cause or clinical significance of these abnormalities in the chronic group is unknown, the common feature of oxygenation or breathing abnormalities suggest that hypoxia-ischemia or related complications may play a key pathogenetic role.

We observed a decrease in [³H]QNB binding to mAChRs in the arcuate nucleus

of a group of SIDS infants compared to infants dying acutely of known causes. We also observed that the age-adjusted mean [³H]QNB binding to mAChRs in several nuclei (including the arcuate nucleus) was decreased in a chronic group with oxygenation and breathing abnormalities compared to SIDS and acute controls. Moreover, the only binding ratios with a significant effect for SIDS versus acute controls were those involving the arcuate nucleus. Together, these findings suggest that mAChR binding is nonspecifically lowered by hypoxia-ischemia or related factors at some point or points in the chronically ill infant's clinical course, whereas it is low in the arcuate nucleus only in the SIDS infant. Experimental studies in animals support the idea that hypoxia-ischemia decreases radioligand binding to brain mAChRs (21). One hypothesis is that the arcuate nucleus is specifically affected in SIDS infants for as yet unknown reasons. Alternatively, the arcuate nucleus may be exquisitely sensitive to hypoxia-ischemia, resulting in its being the only nucleus affected in the presumably milder hypoxic-ischemic events prior to death in the SIDS cases compared to the more severe episodes in the chronic group.

A simple division based on [³H]QNB binding in the arcuate nucleus does not exist between the SIDS and acute control groups, despite a statistically significant difference between the two groups, and the lower 20th percentile of mAChR binding (<75 fmol of tissue per milligram) among the SIDS and acute controls being comprised entirely of SIDS cases. Some overlap and scatter among cases is expected owing to biologic variability. Overlap is also expected because of potential misclassification of cases. It is difficult to classify cases as SIDS or non-SIDS, and classification involves judgment decisions. On occasion, SIDS cases with mild intercurrent illness may be misclassified as acute controls. An-

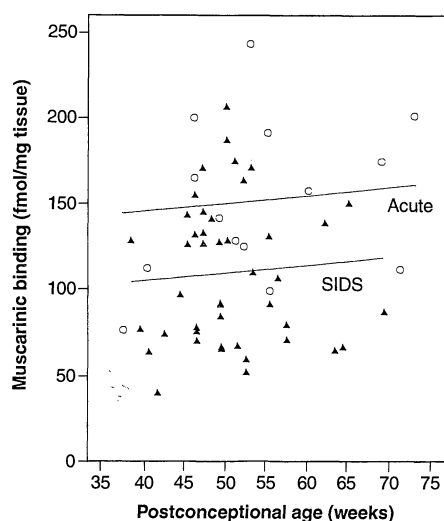


Fig. 2. Scatterplot of raw data and estimated regression lines (model $R^2 = 0.146$; acute controls intercept = 125.83, SIDS intercept = 85.27, age slope = 0.49 fmol of tissue per milligram per week) of mean [^3H]QNB binding to mAChRs in the arcuate nucleus for SIDS cases (solid triangles) and acute controls (open circles) by postconceptional age. Each symbol represents one case. The age-adjusted mean binding level of the SIDS group is significantly lower than that of the acute control group.

other possibility for the overlap between SIDS and acute controls is that SIDS is a heterogeneous group of disorders, in which one group is associated with decreased muscarinic binding in the arcuate nucleus. Finally, neurotransmitters and neuromodulators other than acetylcholine can affect breathing; therefore, although it is possible that acetylcholine is a crucial neurotransmitter, these results do not show that other agents are unimportant or without effect.

The mechanisms resulting in deficient mAChR binding in the arcuate nucleus of the SIDS infants is unknown. In a baseline developmental study (13), we found that [^3H]QNB binding to mAChRs is considerably lower in the arcuate nucleus at mid-gestation and in the perinatal period than in the infant (postnatal) period. Comparing the data of the current study with the baseline developmental study (13), the values of mAChR binding in the SIDS group are more "fetal-like" than "infant-like." These combined data suggest the possibility that there is a disturbance in development of mAChR binding in the arcuate nucleus of the SIDS infants.

The abnormality we now describe in the arcuate nucleus in SIDS infants does not necessarily point to any single cause of SIDS, particularly because the function of the arcuate nucleus in human cardiorespiratory control is uncertain. Moreover, given the small difference (27%) in receptor binding between the SIDS and acute con-

trols, the decreased mAChR binding may be an insensitive marker of a more fundamental mechanism, rather than the cause of cardiorespiratory dysfunction. The evidence in this report is most consistent with the conclusion that a deficiency of mAChR binding in the arcuate nucleus is associated with an increase in the probability of death from SIDS or from chronic disorders of ventilation or oxygenation. An experimental model will be necessary to determine whether this defect is causally linked to SIDS, directly or indirectly.

If the deficiency of mAChR binding in the arcuate nucleus of SIDS infants is causally linked, the precise pathophysiological mechanism resulting in sudden death is unknown. Nevertheless, evidence from experimental animals supports an important role for acetylcholine in regulating central chemoreception and ventilatory drive through its interactions with mAChRs (11, 12). Direct application of cholinergic agonists to the VMS stimulates ventilation, whereas application of antagonists results in decreased ventilation and apnea (11, 12). Moreover, application of the mAChR antagonist atropine to the cat VMS markedly decreases the response to hypercarbia, suggesting that mAChRs accessible to topical application mediate respiratory responses to CO_2 (11). The mAChR may be the chemoreceptor itself (11) or, alternatively, may be located on cells or cell processes involved in chemoreflex pathways (11). A deficiency of mAChR binding in the VMS cell populations could result in an impaired response to a life-threatening challenge of hypercarbia or asphyxia because of decreased number of receptors or binding affinity to acetylcholine (or both).

The question arises as to the nature of the life-threatening challenge in SIDS infants. Although the precise circumstances are unknown, the marked decreases in SIDS rates in countries with programs advocating a change from prone to supine sleeping position (2) support the hypothesis that prone sleeping is causally related to increased SIDS rates. Prone sleeping is associated with spontaneous face-down sleeping position in infants (22). The face-down position is associated with rebreathing exhaled gases and increased end-tidal CO_2 in normal infants (22). This position may also result in upper airway obstruction, either by retropositioning the mandible and occluding the pharynx or by compressing the nose directly (22). We suggest that a normal infant's nervous system detects progressive hypercarbia and asphyxia and responds by arousal and a series of protective reflexes to ensure airway patency, whereas SIDS infants with a VMS defect do not perform these protective reflexes.

REFERENCES AND NOTES

1. M. Willinger, L. S. James, C. Catz, *Pediatr. Pathol.* **11**, 677 (1991).
2. P. J. Fleming *et al.*, *Br. Med. J.* **301**, 85 (1990); A. L. Ponsonby, T. Dwyer, L. E. Gibbons, J. A. Cochran, Y. G. Wang, *N. Engl. J. Med.* **329**, 377 (1993).
3. C. E. Hunt, in *Clinics in Perinatology: Apnea and SIDS*, C. E. Hunt, Ed. (Saunders, Philadelphia, 1992), pp. 757-772.
4. F. G. Issa and J. E. Remmers, *J. Appl. Physiol.* **72**, 439 (1992); R. M. McAllen, *Neuroscience* **18**, 43 (1986); S. Andreatta-Van Leven, D. B. Averill, P. G. Guertzenstein, *J. Physiol.* **421**, 171 (1990); E. N. Bruce, J. Mitra, N. S. Cherniack, J. R. Romaniuk, *Brain Res.* **538**, 211 (1991); N. S. Cherniack, C. Von Euhler, I. Homma, F. F. Kao, *J. Physiol.* **287**, 191 (1979); T. Chonan *et al.*, *Respir. Physiol.* **83**, 77 (1991); T. L. Davidson, M. P. Sullivan, K. E. Swanson, J. M. Adams, *Am. Physiol. Soc.* **74**, 280 (1993); X. W. Dong, D. Gozal, D. Rector, R. M. Harper, *Am. J. Physiol.* **265**, 494 (1993); H. H. Loeschcke, J. DeLattre, M. E. Schlaefke, C. O. Trouth, *Resp. Physiol.* **10**, 184 (1970); N. R. Prabhakar, J. Mitra, E. M. Adams, N. S. Cherniack, *Am. J. Physiol.* **66**, 598 (1989); M. E. Schlaefke, J. F. Kille, H. H. Loeschcke, *Pflueg. Arch.* **378**, 231 (1979).
5. D. E. Millhorn and F. L. Eldridge, *J. Appl. Physiol.* **61**, 1249 (1986).
6. J. L. Feldman and H. H. Ellenberger, *Annu. Rev. Physiol.* **50**, 593 (1988).
7. J. J. Filiano, J. C. Choi, H. C. Kinney, *J. Comp. Neurol.* **293**, 448 (1990). The arcuate nucleus occupies in part a more medial position than the "chemosensitive zones" described in cats. In the cat, neurons that are homologous to human arcuate neurons do not constitute a specific, uniquely named nucleus. In the cat, the arcuate-like neurons occur singly or in clusters of two to four cells, compared to larger clusters of 10 or more neurons in the arcuate nucleus. In the cat and human these neurons about the nucleus reticularis lateralis ventralis caudally and the nucleus paragigantocellularis lateralis rostrally near the lateral medullary surface. In both species, the neurons are associated with a distinct, finely fibrillary neuropil and are intimately opposed to or adjacent to the subpial space. In the ventral midline of the cat, arcuate-like neurons mingle with the ventral portion of the nucleus raphe pallidus and do not form a distinct nucleus. As in the cat, human arcuate neurons are found in ventrolateral, ventromedial, and midline clusters, but because of the large number of neurons in the midline in the human brainstem, the distinction between midline arcuate neurons and human nucleus raphe pallidus is more obvious than in the cat. Previously we emphasized the putative homologous chemosensory role of ventrolateral feline and human arcuate neurons because the experimental literature contains no information on the chemosensory function of arcuate neurons in the midline of the feline medulla along the ventromedian sulcus, that is, the small cell population of the feline midline nucleus raphe pallidus. In cat experiments, neurons in the midline have not been detected previously as chemosensitive, by classical techniques, because the basilar artery lies immediately over the midline structures. Also, neurons lying in the raphe medial to the pyramids may be homologous in their connections, neurotransmitter content, and embryonic origin to neurons near the ventrolateral surface.
8. J. J. Filiano and H. C. Kinney, *J. Neuropathol. Exp. Neurol.* **51**, 394 (1992).
9. D. Gozal *et al.*, *J. Appl. Physiol.* **76**, 2076 (1994).
10. H. Folgering *et al.*, *Bull. Eur. Physiopathol. Respir.* **15**, 659 (1979).
11. E. E. Nattie in *Developmental Neurobiology of Breathing*, G. G. Haddad and J. P. Farber, Eds. (Decker, New York, 1991), pp. 341-71.
12. N. B. Dev and H. H. Loeschcke, *Pflueg. Arch.* **379**, 29 (1979); E. E. Nattie, J. Wood, A. Mega, W. Goritski, *J. Appl. Physiol.* **66**, 1462 (1989); E. E. Nattie and L. Aihua, *ibid.* **69**, 33 (1990); M. D. Burton, D. C. Johnson, H. Kazemi, *Am. J. Physiol.* **66**, 2565 (1989); H. Fleming, M. Burton, D. C. Johnson, H. Kazemi, *ibid.* **71**, 2299 (1991); Y. Fokuda, H. H. Loeschcke, *Pflueg. Arch.* **379**, 125 (1979); R. A. Gillis *et*

- al., *J. Pharmacol. Exp. Ther.* **247**, 765 (1988).
13. H. C. Kinney, A. Panigrahy, L. A. Rava, W. F. White, *J. Comp. Neurol.*, in press.
 14. H. C. Kinney et al., in *Ventral Brainstem Mechanisms and Control of Respiration and Blood Pressure*, O. Trough, R. Millis, H. Kiwull-Schone, M. E. Schlafke, Eds. (Dekker, New York, 1995), pp. 589–609.
 15. Mean postconceptional ages (± 1 SD): SIDS, 51.1 ± 6.8 weeks; acute controls, 55.1 ± 11.0 weeks; and chronic group, 46.2 ± 12.2 ($P = 0.001$). Mean postmortem intervals (± 1 SD): SIDS, 13.5 ± 7.4 hours; acute controls, 11.83 ± 6.8 hours; and chronic group, 9.8 ± 6.9 hours ($P = 0.135$).
 16. We reviewed medical and autopsy records of each case and recorded information about clinical, morphometric, and pathologic characteristics. Information for all variables was not available for every case. To ensure uniform classification of deaths in the study sample, a pediatrician (F.M.) and pediatric pathologist (M.V.-D.) who were blinded to mAChR binding status reviewed the clinicopathologic data recorded from the sudden deaths and classified the case as SIDS or acute control. Causes of death in the acute control group were as follows: acute respiratory infection, 3; myocarditis, 2; enteritis, 1; drowning, 1; accidental asphyxia due to a plastic bag, 1; asymptomatic maple syrup urine disease and sudden death, 1; palliated congenital heart disease with acute intraoperative death, 1; asymptomatic congenital heart disease and sudden death, 2; mild psychomotor retardation, thalamic damage, and sudden death, 1; and noncyanotic chronic lung disease with sudden death from pneumonia, 1.
 17. The causes of death of the chronic controls were as follows: congenital cardiac or pulmonary malformations (or both), 11; primary breathing abnormality, 3; severe perinatal asphyxia, 2; apnea of infancy, 1; and Werdnig-Hoffmann disease with chronic respiratory compromise, 1.
 18. There was a significant difference in sleeping position ($P = 0.046$), with 21/24 (87.5%) of the SIDS infants sleeping prone, compared with 2/5 (40.0%) of the acute group; however, data regarding sleep position were not recorded in the charts for almost half of the SIDS group and over two-thirds of the acute group. Group characteristics were compared by Student's *t* test or the Wilcoxon test for continuous variables, and Fisher's exact test for categorical variables.
 19. J. K. Wamsley, M. S. Lewis, W. S. Young, M. J. Kuhar, *J. Neurosci.* **1**, 176 (1981).
 20. Unfixed, slide-mounted sections were preincubated in 50 mM NaH_2PO_4 (pH 7.4) and 100 mM NaCl for 30 min at room temperature. To determine total binding, we incubated a sample of sections with 1 nM [^3H]QNB (30.1 Ci/mmol, New England Nuclear) in 50 mM NaH_2PO_4 (pH 7.4) and 100 mM NaCl for 2 hours at room temperature. To determine nonspecific binding, we incubated an adjacent subset of sections with 1 nM [^3H]QNB and 1 μM atropine for 2 hours at room temperature. Our procedures for washing and drying the sections and generating the autoradiograms have been described (13). Sections were exposed to [^3H] sensitive film (LKB Ultrafilm- ^3H) for 8 weeks. Each cassette included a set of [^3H] standards (Amersham) for conversion of optical densities to specific activities of ligand bound to tissue in femtomoles per milligram of tissue (fmol/mg tissue). Quantitative densitometry of autoradiographs was performed with a MCID imaging system (Imaging Research, Ontario). Optical densities were converted to specific activities (in fmol/mg tissue) with [^3H] standards. Receptor density was determined in specific nuclei by digitizing the nuclear boundaries directly on the specific activity mosaic displayed on the color monitor, with superimposition of the cell-stained tissue section over the specific activity mosaic, when necessary, with software available on the imaging system. Reference to the cell-stained tissue sections that generated the autoradiograms was made in the determination of the nuclear boundaries. Specific-activity measurements were made in a blinded fashion, without knowledge of clinical diagnosis or postconceptional age. Two sections from four precisely defined levels were analyzed for each nucleus. Measurements were made in the arcuate nucleus at six levels of the medulla. To define the anatomic boundaries of brainstem nuclei, we stained the tissue sections that generated the autoradiograms with cresyl violet or hematoxylin-and-eosin and compared the sections with the autoradiogram. The atlas of Olszewski and Baxter (23) was used as reference. The arcuate neurons are small, round, or multipolar, with eccentric nuclei, prominent nucleoli, and indistinct Nissl substance. They occur in clusters of three or more cells in a fine fibrillary neuropil close to the surface of the lateral and ventrolateral medulla and, in humans, in a larger collection surrounding the ventromedian sulcus. Arcuate neurons are typically found dorsal to the amiculum of the inferior olive, adjacent to the nucleus reticularis lateralis ventralis or nucleus paragigantocellularis lateralis, but ventral to the anterior margin of the spinocerebellar tract, inferior cerebellar peduncle, and spinal tract of the fifth cranial nerve. These correspond closely to cells along the ventrolateral medulla in the cat, which have been associated with respiratory chemosensitive fields. In humans there are abundant arcuate neurons ventral and ventromedial to the inferior olive, contiguous with the larger cells of the nucleus raphe pallidus. Both the ventral and more laterally placed arcuate neurons demonstrate [^3H]QNB binding. The four levels containing the 17 nuclei of interest are defined, with their atlas plate numbers (23) in parentheses: (i) mid-medulla, level of nucleus Roller (Plate XII), for measurements of hypoglossal nucleus, principal inferior olive, nucleus tractus solitarius, and nucleus centralis medullae oblongata; (ii) rostral medulla, level of nucleus praepositus (Plate XIV), for measurements of nucleus gigantocellularis and nucleus paragigantocellularis lateralis; (iii) rostral pons, level of nucleus parabrachialis medialis (Plate X), for nucleus parabrachialis medialis; (iv) rostral pons, level of nucleus parabrachialis lateralis (Plate XXVIII), for measurements of nucleus parabrachialis lateralis, nucleus pontis oralis, paramedian muscarinic bands (13), basis pontis, and locus coeruleus; and (v) caudal midbrain, level of the decussation of the superior cerebellar peduncle (Plate XXXII), for measurements of nucleus cuneiformis, nucleus raphe dorsalis, inferior colliculus, and interpeduncular nucleus.
 21. H. Hara, H. Onodera, H. Kato, T. Araki, K. Kogure, *Brain Res.* **545**, 87 (1991).
 22. B. A. Chiodini and B. T. Thach, *J. Pediatr.* **123**, 686 (1993); J. S. Kemp and B. T. Thach, *N. Engl. J. Med.* **324**, 1858 (1991).
 23. J. Olszewski and D. Baxter, *Cytoarchitecture of the Human Brainstem* (Karger, Basel, ed. 2, 1982).
 24. G. W. Snedecor and W. G. Cochran, *Statistical Methods* (Iowa State Univ. Press, Ames, 1989), pp. 374–397.
 25. We greatly appreciate the technical assistance of L. A. Rava, A. Panigrahy, T. O'Donnell, J. Fleming, and S. Reddy and the statistical help of S. Assmann. We also thank the medical examiners of Boston, MA; Providence, RI; and San Diego, CA, for their help. Supported by the SIDS Alliance, National Institute of Child Health and Human Development (RO1-HD20991), and Children's Hospital Mental Retardation Core Grant (P30-HD18655).

24 February 1995; accepted 7 June 1995